The Growth and Stability of Stress Corrosion Cracks in Large-Diameter BWR Piping

Volume 1: Summary

EPRI

EPRI NP-2472-SY
Volume 1
Project T118-1
Final Report
July 1982

Keywords:
Crack Growth
BWR Pipe Cracking
Intergranular Stress Corrosion Cracking
Fracture Mechanics

Prepared by
General Electric Company
San Jose, California

ELECTRIC POWER RESEARCH INSTITUTE

DISCLAIMER

EPRI-NP--2472-SY Vol. 1

DE82 906435

The Growth and Stability of Stress-Corrosion Cracks in Large-Diameter BWR Piping.
Volume 1. Summary

NP-2472-SY, Volume 1
Research Project T118-1

Final Report, July 1982

Prepared by

GENERAL ELECTRIC COMPANY
Nuclear Engineering Division
175 Curtner Avenue
San Jose, California 95125

Principal Investigators
D. A. Hale
J. D. Heald
R. M. Horn
C. W. Jewett
J. N. Kass
H. S. Mehta
S. Ranganath
S. R. Sharma

Prepared for

BWR Owners Group

and

Electric Power Research Institute
3412 Hillview Avenue
Palo Alto, California 94304

EPRI Project Manager
D. M. Norris

Nuclear Power Division

ORDERING INFORMATION

Requests for copies of this report should be directed to Research Reports Center (RRC), Box 50490, Palo Alto, CA 94303, (415) 965-4081. There is no charge for reports requested by EPRI member utilities and affiliates, contributing nonmembers, U.S. utility associations, U.S. government agencies (federal, state, and local), media, and foreign organizations with which EPRI has an information exchange agreement. On request, RRC will send a catalog of EPRI reports.

NOTICE

Prepared by
General Electric Company
San Jose, California

EPRI PERSPECTIVE

PROJECT DESCRIPTION

This work is part of a four-year BWR Owners Group Program that addresses intergranular stress corrosion cracking (IGSCC) in austenitic stainless steel piping. This project (RPT118-1) considers the safety margin of circumferentially flawed pipe. Volume 1 reports the research in a summary paper format, with the technical details left to the appendixes of Volume 2 that constitute the bulk of this report.

PROJECT OBJECTIVE

The project objectives are (1) to assess the margins of safety, (2) to develop remedies to mitigate cracking, and (3) to apply remedies.

PROJECT RESULTS

This was a good program with results that have high potential for positive impact on the industry. General Electric Company's two-page Executive Summary is a fair evaluation of the accomplishments. An assessment of the major accomplishments are (1) the definition of critical crack size that shows large margins of safety above that given in Section XI of the ASME Code, (2) IGSCC growth-rate design curves that allow end-of-life calculations, and (3) the large pipe test currently under way to verify the analysis.

Douglas M. Norris, Project Manager
Nuclear Power Division

ABSTRACT

This report presents the results of a research program conducted to evaluate the behavior of hypothetical stress corrosion cracks in large diameter austenitic piping. The program included major tasks, a design margin assessment, an evaluation of crack growth and crack arrest, and development of a predictive model. As part of the margin assessment, the program developed diagrams which predicted net section collapse as a function of crack size. In addition, plasticity and dynamic load effects were also considered in evaluating collapse. Analytical methods for evaluating these effects were developed and were benchmarked by dynamic tests of 4-in.-diameter piping. The task of evaluating the growth behavior of stress corrosion cracks focused on developing constant load and cyclic growth rate data that could be used with the predictive model. Secondly, laboratory tests were performed to evaluate the conditions under which growing stress corrosion cracks would arrest when they intersected stress corrosion resistant weld metal. The third task successfully developed a model to predict the behavior of cracks in austenitic piping. This model relies on crack growth data and the critical crack size predicted by the net section collapse approach. Full scale pipe tests were initiated to confirm the model's predictions which in turn could be used to formulate an in-service inspection plan for cracked piping allowing continued plant operation.

ACKNOWLEDGMENTS

The following people made significant technical contributions to this program during its duration:

M. M. Bensch
T. A. Caine
R. M. Chrenko
W. L. Clarke, Jr.
R. L. Cowan
R. B. Davis
J. G. DeBriere
T. P. Diaz
T. Gerber
D. A. Hale
P. P. Hallila
J. D. Heald
R. M. Horn
A. J. Jacobs
C. W. Jewett
J. N. Kass
C. H. Lange
H. S. Mehta
S. Ranganath
P. S. Ryan
S. R. Sharma
W. Vanderputten
S. Yukawa

CONTENTS

Volume 1

CONTENTS

Volume 2

APPENDIXES

ILLUSTRATIONS

TABLES

EXECUTIVE SUMMARY

The research program described in this report investigated the behavior of hypothetical stress corrosion cracks in large diameter austenitic piping. As a result of this work, a method was developed to predict the behavior of cracked pipes. Application of this method demonstrated that very large flaws could be tolerated and as a result showed that a large diameter, welded Type-304 stainless steel pipe, which might contain a stress corrosion crack, has several critical advantages over a small diameter pipe. A large pipe has a more favorable weld residual stress, a weld geometry that would lead to crack arrest, lower sensitization, and a larger wall thickness. The predictions for large pipe can be used to establish an in-service inspection plan for continued plant operation.

The predictive method was supported by several other results. First, failure analysis diagrams for austenitic piping were develped. These diagrams, based on net section collapse, indicate substantial margin to failure in cracked piping under expected conditions and are consistent with experimental and field data. Good agreement with elastic-plastic fracture mechanics predictions was also found. Methods were developed to evaluate the nonlinear dynamic response of a large piping system with a cracked pipe section. These methods were used to quantify the extra structural margin over that determined using linear elastic analysis for piping designed to the ASME Code limits. Thirdly, dynamic pipe tests were performed and confirmed that the elastic-plastic dynamic analysis methods predict the dynamic response of cracked pipe sections. Net section collapse criterion was also confirmed as a conservative estimate of the load capacity of flawed pipes.

As part of the task to evaluate crack growth and crack arrest, finite element methods were developed to better characterize the stress intensity factors for circumferential cracks in pipes subjected to highly nonlinear residual stress distributions. Secondly, laboratory test specimens were used to substantiate arrest of growing stress corrosion cracks in Type-308L weld metal. Constant load crack growth rates, needed for the predictive methodology, were measured

as a function of sensitization in oxygenated high temperature water. Crack growth rates were found to increase with increasing degree of sensitization. Two crack growth rate curves were developed: an expected growth rate curve and a conservative upper bound curve. Cyclic crack growth rates were measured under in-service conditions. The crack growth rate per cycle was a strong function of loading frequency. The growth per cycle increased with decreasing frequency. The cyclic crack growth rates were less dependent on sensitization than those measured under constant load. Finally, confirmatory pipe tests were started in the General Electric Pipe Test Laboratory. Both 4-in.- and 16-in.-diameter pipes, representative of field pipes, are being used to verify the predictive methodology.

Section 1

INTRODUCTION

In late 1974 and early 1975, circumferential cracks were found in a limited number of small diameter Type-304 stainless steel lines in eight operating plants. The origin and significance of these cracks were extensively studied and it was shown that they were due to Intergranular Stress Corrosion Cracking (IGSCC) of the sensitized material in the Heat Affected Zones (HAZs) adjacent to girth welds in the piping (1). Although the cracks posed no safety concern (2), their occurrence was costly because of reactor outages required for pipe inspection and repair.

In the summer of 1978, following discovery of cracks in small diameter piping, IGSCC was found in the T-304 stainless steel large diameter recirculation pipes in one overseas plant. These cracks were shallow part-through-wall cracks. They were not completely circumferential, and were judged to present no new safety concern (3). Because these cracks were the first in large diameter piping (>20"), a reevaluation of the origin and significance of stress corrosion cracks to large pipes was initiated.

Examination of these cracks found in the overseas plant showed that the cracks had initiated immediately adjacent to the fusion line. The IGSCC then traveled through the base metal only a short distance, $\sim$0.100 inch, where it intersected the weld metal due to the weld geometry and appeared to arrest. The duty cycle on the piping was low and the residual stresses due to welding were expected to be lower than those present in small diameter piping.

Following this examination, several factors implied that the plant could have continued operation without removing the large pipes containing the small intergranular cracks. First, arrest of the stress corrosion crack in the weld metal appeared to have taken place. This conclusion was supported by the metallographic studies performed. The HAZ geometry as well as the through-wall residual stresses which became compressive at shallow depths, contributed to this arrest. Secondly, experience had shown that the ductile behavior of stainless steel would allow the

piping to tolerate large deep flaws without severance (4). Finally, the increased wall thickness would allow more crack growth before the crack would reach the critical size.

Since there was both the need and the opportunity to develop the technical basis required to confirm the expected large crack tolerance of stainless steel piping, Electric Power Research Institute (EPRI) and General Electric Company (GE) formulated the program described in this report.

The principal objective of the program would be the development of a methodology for stainless steel piping analogous to the American Society of Mechanical Engineers (ASME) Code Section XI procedures used to evaluate the behavior of flaws in nuclear pressure vessels. This would allow the use of stress reports and information that was readily available.

The analysis methods to be developed over the course of the program would consist of two parts: (1) calculating the allowable flaw size (including an appropriate safety factor) such that component fracture would not occur; and (2) developing methods for predicting crack growth which could be used to evaluate the operating time it would take for an initially discovered flaw to reach the allowable flaw size. The over-all methodology could be used to plan inspection schedules for a large diameter pipe with a detected crack. It would be supported by additional qualitative evidence that the crack would arrest at the weld metal interface.

The program, consistent with this methodology, had two major tasks (5-7). The first effort was aimed at assessing the actual design margin. This approach centered on using static analysis of stresses to determine the locus of flaw configurations that would lead to net section collapse. In addition, plasticity and dynamic load effects were considered in evaluating the safety-margin to failure. The second effort was directed toward the evaluation of crack growth rates and crack arrest in piping. Crack growth rates would be used as inputs into the predictive method for determining the in-service inspection interval. Crack arrest due to interaction with the weld metal would be investigated to provide added conservatism to the crack growth prediction.

The understanding developed by the program would be confirmed by a large diameter pipe test. The methodology synthesized from the major components of the program will be the focus of this final report. The subtasks that contributed the methods, the data, or quantified conservatisms (5-7) will be presented as supporting appendices.

Section 2

THE PREDICTIVE METHODOLOGY FOR EVALUATING THE GROWTH AND STABILITY OF STRESS CORROSION CRACKS IN AUSTENITIC STAINLESS STEEL PIPING

(R. M. Horn, J. N. Kass, and S. Ranganath)

2.1 OVERVIEW

The predictive methodology developed assumes the existence of a circumferential flaw of known maximum depth. The crack is assumed to be in sensitized material so that crack growth due to IGSCC can occur under sustained loads. The methodology has two parts: the determination of an acceptance flaw size that provides adequate safety margin; and a crack growth evaluation to determine the time required for the initial flaw to grow to the acceptance size flaw. Figure 1 displays the important components of this methodology. First, it is necessary to determine the acceptance flaw size. This is based on a critical flaw size that assures leak before break (8,9) and also includes a margin of safety. The safety factor preserves the inherent design margin of piping designed to ASME Code limits. Consideration was also given to the additional margin due to plasticity under dynamic loads. The second task is the evaluation of the growth of the initial flaw to the acceptance size due to the interaction of the stressed material with the environment. Additional conservatisms are present due to the crack's interaction with weld metal which is resistant to environmental cracking.

The results of both parts can then be used to structure a plan for the continued operation of a plant with a component that contains a shallow flaw. The key element of such a plan is an effective, but efficient, in-service inspection program. The specific elements of methodology are as follows:

1. Assessment of design margin in austenitic stainless steel piping.
2. Evaluation of crack growth rates in sensitized stainless steel piping.
3. Application of the predictive method to illustrative field cases.

2.2 ASSESSMENT OF DESIGN MARGIN IN AUSTENITIC STAINLESS STEEL PIPING

2.2.1 Summary

Quasistatic loads on nuclear stainless steel piping include stresses due to pressure, dead weight, and thermal gradients. Unlike ferritic pressure vessel components where failure in the presence of cracks can occur by brittle fracture, the

dominant failure mode in austenitic piping is by plastic instability and collapse. A criterion based on net section collapse has been shown to adequately predict the capability of piping with cracks. Specifically, the net section stress collapse criterion is used by this methodology to evaluate stainless steel piping and safe ends. This criterion assumed that failure is defined by plastic instability which occurs when the stress in the entire net section at the crack reaches the materials' flow stress.

Failure assessment diagrams defining the combination of crack length and depth at which collapse occurs are developed for stress levels expected under normal operation. The diagrams define the critical flaw size. The results show that much larger cracks (including through-wall) than those prescribed by ASME code limits can be tolerated in stainless steel piping. Comparison of the analytical prediction with experimental data on pipes with cracks verifies this approach.

For dynamic loads such as seismic, water hammer, and safety/relief valve actuation, piping analysis is generally performed assuming linear elastic behavior. While this is acceptable for the analysis of uncracked piping, it is overly conservative for the evaluation of cracked piping components. Because of plastic deformation at the cracked section, the actual stresses in a cracked pipe are much smaller than those predicted by elastic analysis. Thus, by performing an inelastic system analysis, much higher margins (compared to that indicated by conventional elastic analysis) are demonstrated. The inherent margin due to plastic deformation in a cracked piping system under dynamic loads is illustrated by an elastic-plastic analysis of a dynamic pipe test configuration. It is shown that elastic analysis currently performed in ASME Code piping evaluations significantly underestimates safety margins in cracked pipes. This establishes that the failure diagram developed for faulted conditions is conservative.

The net section stress collapse criterion has been applied to establish the locus of crack depth/crack length combinations for a given load that produce plastic instability. However, to ensure additional margin, an acceptance flaw of size a_c must be determined. Development of this acceptance flaw as a function of load is performed using safety factors that are consistent with ASME Code procedures. The acceptance flaws are then presented in table form for normal conditions and faulted conditions.

2.2.2 Evaluation of Cracked Pipes for Static Loads

This section discusses the evaluation of the margin in cracked pipes for static primary loads such as pressure and bending stress that exist under normal operation.

2.2.2.1 Analysis Using the Net Section Collapse Criterion. For materials where brittle fracture is a failure mode, the critical flaw parameters can be determined on the basis of linear elastic fracture mechanics (LEFM). However, for ductile materials like stainless steel, failure criteria based on LEFM are not valid since failure is characterized by gross yielding and subsequent plastic instability. In the analysis presented here, failure is predicted using the net section collapse criterion. It is assumed that a pipe with a circumferential crack is at the point of incipient failure when the net section at the crack forms a plastic hinge. The material is assumed to be rigid - perfectly plastic with plastic flow assumed to occur at a critical stress level, σ_f, called the flow stress of the material. The criterion is simple to apply and has been shown to be effective in predicting failure of stainless steel pipes containing circumferential cracks (10,11). To determine the point at which collapse occurs, it is necessary to apply the equations of equilibrium assuming that the cracked section behaves like a hinge. For this condition, the stress state and the cracked section is as shown in Figure 2, where the maximum stress is the flow stress of the material, σ_f. Let P_m be the primary membrane stress in the longitudinal direction in the uncracked section of the pipe and P_b be the primary bending stress and consider a circumferential crack of length, ℓ, and constant depth, d, located on the inside surface of a pipe (Figure 2). Equilibrium of longitudinal forces and moments about the axis gives the following equations:

Case 1: Neutral axis located such that $\alpha + \beta < \pi$

$$\beta = \frac{(\pi - \alpha\, d/t) - (P_m/\sigma_f)\pi}{2}$$

$$P_b = \frac{2\sigma_f}{\pi} (2 \text{ Sin } \beta - d/t \text{ Sin } \alpha) \qquad (1)$$

Case 2: Neutral axis located such that $\alpha + \beta > \pi$ (assume crack takes compression)

$$\beta = \frac{\pi\,(1 - d/t - P_m/\sigma_f)}{2 - d/t}$$

$$P_b = \frac{2\sigma_f}{\pi} (2 - d/t) \text{ Sin } \beta \qquad (2)$$

where t = pipe thickness and α = half the crack angle as shown in Figure 2, and β defines the location of the neutral axis. The above equations together define the combinations of α and d/t for which failure by collapse is predicted under the given applied stresses P_m and P_b. It should be noted that secondary and peak stresses have no effect on the limit load because they are produced by the action of imposed strains or are locally confined and are self-limiting and, therefore, are not included in the analysis. These equations can be solved by considering a given value of crack depth and determining the angle α at which failure occurs for specified values of P_m, P_b, and σ_f. The flow stress, σ_f, a function of the yield stress, S_y and ultimate stress, S_u of the material and is assumed here to be a material property.

Figure 3 shows a failure analysis diagram developed for stainless steel piping with the curves shown for two stress levels - one corresponding to the design condition which included limiting earthquake loads. The value of flow stress was assumed as 48.0 ksi based on experimental data. For the normal operation condition, the primary stress of interest is the axial membrane stress due to internal pressure. This stress was assumed to be 6 ksi (Pr/2t). Other primary stresses were negligible. For the design conditions (which includes the operating basis seismic loads), the ASME Code stress limit is $(P_m + P_b) = 1.5\ S_m$ (S_m for stainless steel at 550°F = 16.9 ksi). It should be noted that this is the maximum stress permitted by the Code and, in reality, the calculated stresses are usually well below the Code limits.

The failure analysis diagram of Figure 3 indicates that stainless steel pipes can tolerate large circumferential cracks without failure. For example, under normal operating condition, a through-wall crack extending around 55% of the circumference will not lead to collapse. This is consistent with field experience with stainless steel piping in BWR operation.

2.2.2.2 Comparison with Field Experience and Experimental Data. Available field observed data on circumferential cracks in welded austenitic pipes and safe ends is also shown on the failure analysis diagram (Figure 3) in order to make a qualitative estimate of typical safety margins. It is seen that the field data on cracks is well within the safe region. Moreover, the data shows a very strong tendency for the pipe to leak before the collapse load point is reached, thus indicating a strong trend for a "leak before break" condition. Analysis presented in Appendix D supports

this field experience. Comparisons of the analytical predictions with experimental data from GE pipe tests under axial loading as well as test data reported by Reynolds (12) have shown that the net section collapse criterion predicts failure margin of pipes with cracks conservatively. Also, since actual stress corrosion cracks have varying depths and are seldom aligned in the same plane, the idealized representation used here would enhance the conservatism.

2.2.2.3 Discussion. The net section collapse criterion discussed here is consistent with the ASME Code approach based on limit design analysis. Therefore, stresses reported in ASME Code stress reports can be directly used in assessing the margin of pipes with cracks. Although the criteria used here are based on collapse theory, Smith (13) has shown that the existence of a critical net section stress for crack initiation in a center cracked panel can be justified by using results from a detailed general yield fracture mechanics analysis. By relating the crack opening displacement to the critical net section stress, he concluded that except for a weak dependence on panel width (corresponding to pipe diameter), the net section stress at crack initiation is essentially constant for a wide range of crack depth-to-width ratios in a highly ductile material like stainless steel. A limit load approach based on flow stress has also been used in the British two-parameter approach (14) and in the analysis of longitudinal cracks in pressurized piping (15).

The details of the development of the failure analysis diagrams are given in Appendix A. This appendix explores the development of the diagrams for Inconel as well as for stainless steel, the effect of considering variable depth cracks and compound cracks, comparison with experiments as well as field data, and sensitivity of the failure predictions to the assumed flow stress. The general methodology can be applied for all shapes of circumferential cracks.

2.2.3 Evaluation of Cracked Pipes for Dynamic Loads

In general, the largest stresses in piping come from the dynamic loads due to design basis earthquakes, water hammer, and safety/relief valve actuation. The stresses due to these loads are calculated using dynamic analysis based on linear elastic behavior. This is acceptable for the uncracked piping system since inelastic behavior is not expected under the applied dynamic loads. However, in a cracked pipe, plastic deformation is likely to occur at the cracked section and the actual stress at the cracked section is much smaller than that predicted by linear elastic analysis. Therefore, assessments based on stresses reported in ASME Code piping stress reports would underpredict

the safety margin in pipes. This inherent margin has been illustrated by an elastic-plastic dynamic analysis of a cracked piping system subjected to anchor point motions. It has been shown that the actual moment at the cracked sections is lower than that predicted by elastic analysis and that much higher anchor point motions can be tolerated without failure. This work is reported in Appendices B and C.

Appendix B details analysis methods to evaluate the inherent margin. Typical piping systems are analyzed with seismic load time histories to illustrate the additional margins. Appendix C details actual pipe tests performed to experimentally benchmark the method and verify this margin.

The elastic-plastic analysis method consists of two steps:

1. Stiffness Evaluation of the Cracked Pipe Element: In order to correctly model the effect of the crack on the response of the piping system, it is necessary to characterize the local stiffness of the cracked pipe element. This stiffness can then be included in the dynamic analysis model of the total piping system to determine the over-all response. The moment-curvature relationship for the cracked pipe element is determined by performing a three-dimensional finite element analysis of the pipe segment under moment loading using the ADINA structural analysis finite-element computer program.

2. Elastic-Plastic Dynamic Analysis: The elastic-plastic dynamic analysis is performed using a GE computer program based on the component element method of dynamic analysis. In the dynamic model of the test configuration, the cracked pipe is represented by a pipe element with stiffness properties determined in step (1) above. The dynamic response is then evaluated for different input values of support exitation amplitude (forces and/or displacements). The maximum moment at the cracked section can be determined assuming a stationary crack.

2.2.3.1 Dynamic Pipe Tests. For these tests, the input excitation were sinusoidally varying support displacements as discussed in Appendix C. Figure 4 shows the moment at the cracked section as a function of support motion amplitude for the dynamic pipe tests. For small excitation, the behavior is elastic but as the support motion goes up, it is seen that plasticity at the cracked section becomes important and the stress is significantly lower than that predicted by elastic analysis alone. The collapse moment for this cross section is approximately 120 in.-kip for an assumed linear elastic behavior; this collapse moment would have been reached at under 0.03 in. of support motion. On the other hand, the elastic-plastic dynamic analysis would predict collapse at approximately 0.06 in. of excitation. The ratio of the two predictions of the support motion required for

collapse - a factor of two in this example - is a measure of the additional margin that is inherently available in a cracked pipe. In general, the additional margin increased as the excitation increases.

Figure 4 also shows results obtained from two of the tests detailed in Appendix C with 4-in. Schedule 80 piping with 360-deg circumferential cracks of depth equal to two-thirds of the wall thickness. The two tests (one on Type-304 stainless steel pipe and the other with Inconel pipe) show behavior consistent with the analytical predictions of elastic-plastic analysis. The additional margins in these cases were 4 and 3, respectively. The test data, therefore, confirms the additional margin under dynamic loading due to the effects of crack plasticity. Since some fatigue growth occurred at the notch section prior to failure, the net section at collapse was somewhat smaller than the initial value. This indicates that the actual margin in the tests was even higher.

2.2.3.2 Analysis of Total Piping System. These methods were also used to analyze a total piping system containing a crack as described fully in Appendix B. The model used represented an entire recirculation system containing a crack. Input excitation based on seismic time histories were used. Table 1 gives a summary of the analysis results for various cases of flaw configuration, flaw location and seismic input combinations. The results are analogous to those obtained for the simpler dynamic pipe test results with substantial margins demonstrated.

2.2.3.3 Discussion. The analysis of a piping system for a seismic event essentially involves applying the expected anchor point motions at the support points and performing a linear elastic dynamic analysis. This approach is overly conservative for a system with cracks since there is a significant amount of plasticity at the crack location. This concept is illustrated by a combined analytical/experimental evaluation of a dynamic pipe test configuration with cracks in a piping system (Appendix B). It is shown that elastic analysis would predict failures at much lower support excitation compared to the elastic-plastic analysis. The ratio of the two predictions is a measure of the additional margin in a cracked pipe under dynamic loading. The excellent agreement of the analytical predictions with test data on cracked stainless steel and Inconel piping further confirms the additional margin due to plasticity effects that are not included in conventional ASME Code analysis.

The analysis and data supports the use of the net section collapse-based failure analysis diagrams where all loads are treated statically.

2.2.4 Development of Acceptance Criteria for Cracked Piping

The net section collapse approach permits the determination of the critical flaw size in a stainless steel pipe for a given combination of applied stresses. However, the acceptance flaw size is smaller than this and can be determined by applying a required safety margin on the failure flaw parameters. The acceptance flaw size, a_f, is the maximum size to which a detected flaw can be allowed to grow without the need for repair. In other words, it is the maximum allowable end-of-inspection period flaw size. In order to develop easy-to-apply acceptance flaw tables, the following simplifying assumptions are made.

2.2.4.1 Membrane Stress. In calculating the location of the neutral axis (angle β in Equations 1 and 2), the value of the primary membrane stress is required. Since pipes are generally sized such that the hoop stress at design pressure is less than S_m (ASME Code Section III, NB-3640) it is reasonable to assume that the axial membrane stress P_m is $S_m/2$. Parametric studies with different values for P_m have shown that the allowable flaw sizes are not significantly dependent on the assumed value of P_m.

2.2.4.2 Flow Stress. Experimental measurements (10) and evaluations of GE pipe test data indicate that the assumption of $\sigma_f = 3S_m$ is reasonable. This is slightly higher than the average of the Code minimum values of the ultimate strength and yield strength at 550°F for Type-304 stainless steel. A flow stress value indexed to S_m is more realistic since different grades of austenitic materials have different strength properties and pipes are designed on the basis of the design stress intensity S_m. Also, the Code minimum properties are for annealed material and do not consider the beneficial effects of strain hardening. In the vicinity of piping welds where cracks are likely to occur, the strength of the weld HAZ is expected to be higher than that of the annealed material. In view of the above reasons, the assumption $\sigma_f = 3S_m$ is reasonable.

2.2.4.3 Safety Factor. The philosophy in setting the acceptance standards is to preserve the minimum safety margin inherent in the ASME Code design basis for uncracked piping. For normal conditions the minimum margin on primary membrane stress is 3 ($P_m < S_m$ where S_m is the lower of $S_u/3$ or $0.9\ S_y$). For bending stresses in piping, the margin is slightly lower as seen from Equation 9 from NB-3600 for straight piping:

$$P_m + P_b \leq 1.5\ S_m \qquad (3)$$

where P = pressure, t = thickness, D = outside diameter, and M is the applied moment including seismic loading.

Considering the case of pure moment loading alone it is seen that the total safety margin arises from two factors: (1) ratio of 2 coming from the allowable limit of 1.5 S_m whereas the flow stress is $3S_m$ and (2) the ratio of the fully plastic moment for a thin pipe ($4\ \sigma_f\ r^2\ t$) to the moment for just reaching the flow stress on the surface ($\pi\ \sigma_f\ r^2\ t$) giving a factor of $4/\pi$. (For rectangular cross sections the ratio is 1.5.)

Thus, for pipes in bending the over-all safety margin is $8/\pi = 2.546$. In setting up the acceptance standards the safety margin will be imposed on $P_m + P_b$. The required safety factor is the average of the Code minimum safety margins for P_m and P_b = 1/2 (3.0 + 2.546) = 2.773.

For faulted conditions, the safety margin is one-half of the value for normal conditions, i.e., 1/2 (2.773) = 1.387. This is also consistent with the Code design basis since the allowable limit in Equation 3 is $3S_m$ for faulted conditions.

Based on the above assumptions, flaw assessment diagrams can be developed for different values of P_m+P_b (P_m is assumed to be $S_m/2$ and $\sigma_f = 3S_m$). Figure 5 shows the failure diagram for $P_m+P_b = S_m$. The dotted line represents the combination of flaw depth and length defining plastic instability. Applying a safety factor of 2.773 on $P_m + P_b$ the allowable flaw parameters can also be calculated as shown in the dark line. Flaw combinations below this line will preserve the minimum safety margins of the ASME Code. Since through-wall cracks cannot be tolerated (even though sufficient structural margins can be demonstrated) a piecewise linear representation is proposed to determine the allowable flaw sizes. Essentially it assumes that flaws exceeding 50% of the circumference are equivalent to a 360° circumferential crack. Cracks less than 50% are governed by the 45° line as shown in Figure 5. However, the maximum allowable crack depth is limited to 75% of the wall thickness in order to be consistent with Appendix A of Section XI, ASME Code which requires the crack arrest depth in pressure vessels to be less than 75% of the wall thickness. Also, from a practical perspective it may be more cost effective to repair/replace the pipe for such deep cracks even though adequate structural margins can be shown. The linear approximation provides a simple conservative method of determining allowable flaw depth and lengths based on the allowable flaw depth for a 360-deg circumferential crack. The allowable flaw depth for a 360-deg

crack can be determined using Equation 2 and applying a safety factor of 2.773 on $P_m + P_b$. For crack lengths less than 50% of the circumference the 45-deg line can be used. Similar diagrams can also be developed for emergency and faulted conditions except that the required safety margin is 1.387.

The acceptance flaw sizes shown in Figure 5 can be determined for a range of applied stresses for both normal and faulted conditions. Tables 2 and 3 show the allowable values for different values of $(P_m+P_b)/S_m$ for normal and faulted conditions. For conservatism, the maximum allowable crack depth for a 360-deg flaw was restricted to be less than 50% of the wall thickness. For intermediate values of P_m+P_b the acceptance flaw sizes can be determined by interpolation.

The methodology presented here for evaluating cracks is based on limit load design concepts which are strictly valid with highly ductile materials. They do not explicitly consider failure by brittle fracture or tearing instability. To preclude brittle fracture concerns, the criteria outlined here are restricted to austenitic piping and the associated weld materials and stainless steel castings with low ferrite content. Although tearing instability is not explicitly considered here, tearing instability is not likely since the acceptance criteria developed here assure large margins over hinge formation.

It should be noted that the acceptance criteria, a_f, represent the maximum flaw size that can be tolerated at the end of the next inspection interval. To determine the allowable value, a_i, at the previous inspection, it is necessary to subtract the expected crack growth during that interval. The next section discusses the method to be used to make calculations of growth for stress corrosion cracks.

In summary, the proposed acceptance criteria are based on the net section collapse approach. This is consistent with the design basis for piping which is derived from limit load concepts. The proposed criteria assure that the minimum safety margins required by the ASME Code are preserved during operation. Another advantage comes from the fact that no special stress analysis or fracture evaluation is required to determine flaw acceptability. Information that is already available in piping stress reports can be used to make the assessment. Specific material properties such as J_{Ic} data, tearing modulus and J-R curves are not needed for the evaluation. The only material property needed is the flow stress which can be obtained from minimum strength properties specified in the Code. Thus, the proposed criteria offer a simple, conservative method for assessing flaws in piping.

2.3 EVALUATION OF CRACK GROWTH IN LARGE DIAMETER SENSITIZED STAINLESS STEEL PIPING

2.3.1 Summary

The time interval between two successive inspections cannot exceed the time required for the initial flaw to grow to the acceptance flaw size. The calculated crack growth under operating conditions, Δa, can be used to establish the appropriate time increment between inspections. The methodology for determining the growth of the flaw is described in this section. It uses LEFM to determine the stress intensity factor at the crack tip and includes residual stress as well as other applied loads. The assumption is made that the stress intensity factor, K, is the principal factor controlling the rate of crack growth. It is a function of the flaw geometry, component geometry, and the stresses. Crack growth rates as a function of stress intensity were determined from laboratory data and are used for the crack growth predictions. The crack growth rates depend on material condition, loading history and environment. To establish an initial in-service inspection plan, upper bound crack growth rates are generally used to assure the most rapid estimate of crack deepening. These upper bound rates have been derived from tests performed in severely sensitized material, in a condition expected to be worse than that in as-welded pipe. At the first inspection, true estimates of the crack growth behavior in the cracked pipe can be made and can be used to reevaluate the future in-service inspection plan. This behavior would be expected to be similar to that predicted by the representative crack growth data that has been used to predict field experience accurately. The expected slower crack advancement would lead, in turn, to longer times between inspection.

2.3.2 Assessment of the Stress Intensity in Large Diameter Piping

The first task in the crack growth evaluation is the determination of the crack growth driving force, the stress intensity factor, K. This factor depends on the stresses present in the pipe. For pipes which have been sensitized by the girth welding process, a circumferential sensitized region would be developed and would be the site of IGSCC. The stress intensity factor due to the axial stresses control the environmental crack growth process. Longitudinal cracking would not be expected in large pipes because of the limited longitudinal extent of the sensitization and because the stress state driving crack growth would be lower in the hoop direction.

The total stress state to be considered results from different imposed loads, and strains. External imposed loads such as pressure and dead weight lead to stresses the magnitude and distribution of which are governed entirely by equilibrum

considerations. The action of strains resulting from support displacements also produce stresses. However, these strains are governed entirely by displacement continuity requirements and are therefore self-limiting. Thermal stresses are of this type. Finally, pipe welding can produce self-equilibrating residual stresses. These stresses are influenced by a variety of factors and in turn can vary as to through-wall distribution and magnitude.

For a piping system of interest, the stresses resulting from loads and displacements can be obtained from design reports. Example values are given in Reference 6. Through-wall residual stresses from welding for a specific pipe must be based on data from previous measurements made on piping of a similar size.

Appendix E details residual stress distributions for large pipes ($\geq$20 in. diameter). These residual stresses are tensile on the i.d. and become compressive at $\sim$15% of the wall thickness.

Transient stresses, except for those developed during startup, contribute only to fatigue crack growth and not to IGSCC. For the transients associated with normal operation, crack growth is small and will not be included. The role of startup will be discussed later with crack growth rate data.

Using the information on the stresses arising from imposed loads, strains, and welding, the crack driving force, K, can be determined. Two conservative assumptions are made. First, the different stress contributions are superposed consistent with linear elastic methods used by ASME Code. This is conservative in that stresses higher than the yield stress would be calculated. The second conservatism is the assumption that the crack is a 360-deg circumferential crack, allowing two-dimensional finite element methods to be used to estimate the stress intensity factor. The specific stress intensity solutions used were either developed by Buchalet and Bamford for a 360-deg circumferential flaw in a pipe with a r/t ratio of 10 (16) or developed as part of this program. The special stress intensity solution for large pipe weld residual stress is detailed in Appendix F along with the applicability of the superposition principle in developing stress intensity factors for pipes.

2.3.3 Assessment of the Intergranular Stress Corrosion Crack Growth Rates in Large Diameter Piping

In order to assess the size of an intergranular stress corrosion crack with time, it is necessary to evaluate the crack growth rates for the material under the service environment and service loading conditions. The growth rates are a function of the sensitization level present in the material at the heat-affected zone location where the intergranular crack is situated. Figure 6 displays this location in cross section. The position of the crack in relation to the nonsensitized weld metal is also displayed. While there is high likelihood that the crack will slow down or arrest due to its interaction with the weld metal, as discussed in Appendix G, crack growth rate evaluation is made ignoring this intersection. Crack growth rates for several conditions, listed below, were determined during the course of the program using laboratory specimens. The data conditions are as follows:

1. Constant applied load, 8 ppm O_2 high temperature water environment
2. Constant applied load, 0.2, ppm O_2 high temperature water environment
3. Slow rising load, 8 ppm O_2 high temperature water environment
4. Slow rising load, 0.2 ppm O_2 high temperature water environment
5. Cyclic loading (at several frequencies) 0.2 ppm O_2 environment.

The tests were conducted in fracture mechanics type specimens which were sensitized to different levels using isothermal heat treatments. Two heat treatments were emphasized: a heat treatment of 2 hours at 1150°F representative of weld sensitization, and one of 24 hours at 1150°F representative of severe furnace sensitization. The work is detailed in Appendix H. Upon completion of the testing program, the test data, along with data developed by other investigators, were used to predict crack growth in pipes.

2.3.3.1 Constant Load Crack Growth Rate Data. The stress state in piping under service conditions remains almost unchanged for most of the design life. Therefore, crack growth rate data for sustained load can be used to make field predictions. Crack growth rate data for sustained load was separated into two categories (Appendix H): (1) representative crack growth rates, and (2) upper bound crack growth rates.

To determine the realistic estimate of the crack growth rates in large diameter pipe material, the representative data is appropriate (17). The sensitization level and

environmental conditions are similar for the large pipe during operation to that of the laboratory tests used to produce the representative data. This is discussed in Appendix I. Upper bound accelerated crack growth rates are most appropriate where furnace sensitization was induced through a post weld heat treatment in the piping or safe end material. The crack growth rate data is given in Appendix H as a function of the stress intensity factor.

2.3.3.2 Cyclic Crack Growth Rates. In addition to constant loads, the piping experiences slow increasing loading during startup as well as changes in loading of short duration under transient conditions. The cyclic crack growth rates have also been investigated and are discussed in Appendix H. This work established that IGSCC is only observed at slow loading rates (loading from the minimum to maximum stress over a period in excess of several minutes). For recirculation piping systems, these slow loading rates are only experienced during startup. The number of startups over a year period is on the order of 1 to 10. Using the cyclic crack growth results of Appendix H would lead to growth of less than 0.001 in. per year. Therefore, evaluations of crack growth only take into account the significantly larger amount of growth occurring under steady state constant load conditions.

2.3.4 Crack Growth Evaluation Curves

Two curves were derived from the constant load data as shown in Figure 7. The first curve, presented in Reference 6, bounds all the constant load data. The data on or near this curve were generated in material that was severely sensitized and in most cases exposed to high coolant oxygen. In addition, the majority of tests were conducted at high stress intensities producing significant plasticity in front of the crack tip which could enhance ISCCC rates. This curve has been labeled "Upper Bound Evaluation Curve" and as discussed in Subsection 2.4 is most useful in establishing a conservative, bounding estimate of crack growth for the initial application of the methodology. This prediction would lead to the shortest inspection interval. It could also be used when sensitization due to post weld heat treatment or other treatment would be known to be high.

The second curve, the "Representative Evaluation Curve," is useful in predicting actual behavior of pipe sensitized by the welding process. The basis of this curve was data obtained in Type-304 stainless steel sensitized to a level representative of weld sensitization by a 1150°F, 2-hr isothermal heat treatment. The testing was conducted in 0.2 ppm O_2 high temperature water, conditions characteristic of normal plant operation. This representative curve has two features that are typical of stress corrosion crack growth curves - a threshold stress intensity and a plateau

crack growth rate (6). As the data base increases, this curve position might be expected to shift. However, the curve shape would be expected to remain similar and the absolute position would fall below the upper bound data. The lower representative curve is not as strongly supported by the data as is the upper bound curve. However, as demonstrated in the summary, this data is the basis for predictions that explain field experience very well as discussed in Subsection 2.4.3.

2.4 APPLICATION OF PREDICTIVE METHODOLOGY

2.4.1 Summary

The predictive methodology will be used to model behavior of pipes in operating plants. In addition, to check its reliability, sample field cases have been selected for trial application. In the first section, the predictive model is applied to a representative field large diameter pipe. Predictions of acceptable flaw size and growth of an initial flaw to the acceptance criterion are made. In the second section, predictions of times to failure are made for two classes of pipes and the predictions are compared with average times to failure from field experience. To further calibrate the model, a specific field failure is examined and it is shown that the method leads to reasonable predictions of pipe lifetimes.

2.4.2 Predictive Methodology Application: Large Diameter Pipe

The first part of the methodology is the determination of the acceptable crack size. Representative stresses, given in Reference 6, are used for the analysis. Figure 8 gives the locus of flaw size for net section collapse, for stress levels typical of normal operation. This was calculated for an assumed flow stress of 48 ksi. Consistent with Section 2, the acceptance criterion for the end-of-inspection period flaw is displayed. The methodology for crack growth investigates the growth of only the worst flaw shape, the 360-deg circumferential flaw, which must reach 50% in depth before it exceeds the acceptance criterion. Figure 9 shows the crack size as a function of time for an initial flaw, 0.065 in. deep or 5% of the 26-in. Schedule 80 pipe used as the example. Both the Representative Evaluation Curve and the Upper Bound Evaluation Curve were used to predict crack growth. It is evident that the crack will grow to 35% of the wall in 174,000 hours (roughly 23 years) or a growth of 0.015 inch/year based on representative growth rates. The crack will not be expected to reach the acceptance flaw size because (1) the stress intensity would fall below the threshold value for IGSCC and (2) the growing crack would intersect the weld metal and arrest. Figure 9 also displays the crack depth versus time predictions made using the Upper Bound Evaluation Curve. These predictions were presented earlier in Reference 6. Although the upper bound

predictions are much higher, the crack still does not reach the 35% depth until 2 years. The methodology clearly demonstrates that continued operation of large pipes is possible with reasonable inspection programs even with conservative crack growth rate assumptions. An initial inspection at 18 months after detection would allow sufficient margin, with future inspections dependent on the results of the first inspection. If the observed crack growth is less than the predicted Upper Bound value as expected, a decreased inspection frequency can be justified. Methods for setting up an inspection plan are discussed in Appendix J.

2.4.3 Predictive Methodology Verification: Application to Field Failures

2.4.3.1 Representative 4-in.- and 10-in.-Diameter Pipe Behavior. The methodology was applied to past field failures in small diameter weld sensitized Type-304 stainless steel lines to confirm its accuracy. Predictions were compared to the occurrences of actual IGSCC failures. In order to predict the general behavior of field incidents, nominal operating stresses and weld residual stress distributions were assumed. The nominal sustained stress was assumed to be 11.5 ksi or 2/3 S_m. This consists of 6 ksi primary stress and 5.5 ksi secondary stress. A linear varying weld residual stress from 40 ksi on the i.d. surface to -40 ksi on the o.d. surface was assumed. This is consistent with values reported in earlier studies, for small diameter pipe (1,6). The initial flaw was assumed to be 0.010 in., small enough to preclude any initiation time considerations. The representative crack growth rate curve shown in Figure 7 was used. Figure 10 shows the predicted crack growth of a circumferential crack as a function of time for 4-in. Schedule 80 pipe. At 43,000 hours, the crack has reached ~60% of the total pipe depth. At this point, it is expected that leakage will occur shortly thereafter, since the rate of growth is rapid and since the nonsymmetric stress distribution would cause preferential crack growth to through wall. To compare the predictions with field failures, times to failures in 33 pipe cracking incidents were reviewed (1,18). (Only pipes which had through-wall cracks were considered.) The average operation time was calculated based on plant availability. The shortest, average, and longest times to failure for the 4-in. pipe are plotted on Figure 10. The predicted failure time of the pipe matches the average time to failure from the field data. If the upper bound crack growth rate data from Figure 7 was used, then the model would easily account for the shortest time to failure. This great variability would be more expected to exist with small diameter piping due to the wide variation in degree of sensitization possible with field welding procedures. Similarly, the prediction for nominal 10-in. Schedule 80 pipe is displayed in Figure 11. As

before, nominal values of the primary, secondary, and residual stresses components were assumed. A starting flaw of 0.010 in. was used. The crack reaches ~60% of the wall at a time of 44,000 hours. The field experience (18) is also shown in Figure 11. The shortest, average, and longest operation time are given. As with the 4-in. Schedule 80 pipe predictions, the predictions made using representative crack growth rates match the average time failure from field data. Predictions of the representative behavior of 4-in. Schedule 80 and 10-in. Schedule 80 and the good agreement with field cracking experience verifies the methodology and its ability to predict IGSCC failure time for sensitized pipes.

2.4.3.2 10-in. Schedule 80 Recirculation Riser: Specific Application. To further calibrate the predictive methods, a specific cracking incident was selected and failure times predictions were made using the actual stresses (instead of nominal data in the previous example). Table 4 characterizes the stresses present in a 10-in. Schedule 80 recirculation riser, where IGSCC failure occurred in 25,900 hours. Since the pipe had experienced a large thermal gradient during operation, a thermal stress was added to the pressure stress and a linear bending residual stress distribution. Figure 12 shows the predicted crack depth as a function of time. The crack reaches 60% depth at 22,000 hours, compared to the actual failure time of 25,900 hours. The close agreement between the predictions and the actual failure time further support the reasonableness of the predictive methodology and underlying data base.

2.5 CONCLUSIONS: GROWTH AND STABILITY OF STRESS CORROSION CRACKS IN AUSTENITIC STAINLESS STEEL PIPING

The major accomplishments are as follows:

- Failure Analysis Diagrams for austenitic piping were developed. These diagrams, based on net section collapse, indicate substantial margin over ASME Code limits to failure in cracked piping under expected conditions. These analytical predictions are consistent with experimental and field data and show good agreement with elastic-plastic fracture mechanics predictions.

- Methods were developed to evaluate the nonlinear dynamic response of a large piping system with a cracked pipe section. These methods were used to demonstrate the extra structural margin over that determined using linear elastic analysis for piping designed to the ASME Code limits.

- Dynamic pipe tests were performed and confirmed that the elastic-plastic dynamic analysis methods predict the dynamic response of cracked pipe sections. These tests also confirmed that net section collapse criteria can be used as a conservative estimate of the load capacity of flawed pipes.

- Finite element methods were developed to better characterize the stress intensity factors for circumferential cracks in pipes subjected to highly nonlinear residual stress distributions.

- Laboratory test specimens were used to substantiate arrest of a growing stress corrosion crack in Type-308L weld metal.

- Constant load crack growth rates, needed for the predictive methodology, were measured as a function of sensitization in oxygenated high temperature water. Crack growth rates were found to increase with increasing degree of sensitization. Two crack growth rate curves were developed: an expected growth rate curve and a conservative upper bound curve.

- Cyclic crack growth rates were measured under in-service conditions. The crack growth rate per cycle was a strong function of loading frequency. The growth per cycle increased with decreasing frequency. The cyclic crack growth rates were less dependent on sensitization than those measured under constant load.

- Confirmatory pipe tests were started in the General Electric Pipe Test Laboratory. Both 4-in.- and 16-in.-diameter pipes, representative of field pipes, will be used to verify the predictive methodology.

The key conclusions drawn from the application of the methodology are summarized as follows:

- The Failure Analysis Diagram shows that piping systems designed to ASME Code stress limits can have very large flaw tolerances.

- The Failure Analysis Diagram is both a realistic and practical way to evaluate margin for cracked pipe sections and can be used in conjunction with a crack growth model to establish a specific In-Service Inspection plan.

- Large diameter welded Type-304 stainless steel pipes which contain stress corrosion cracks have several critical advantages over small diameter pipes. These pipes have more favorable weld residual stresses and weld geometry, lower sensitization, and larger wall thickness. These features allow the use of predictive methods to establish an In-Service Inspection plan for continued plant operation.

2.6 REFERENCES

1. H. H. Klepfer, et al., "Cause of Cracking in Austenitic Stainless Steel Piping," General Electric Company, 1975 (NEDO-2100).

2. "Technical Report on Material Selection and Processing Guidelines for BWR Coolant Pressure Boundary Piping," U.S. Nuclear Regulatory Commission, July 1977 (NUREG-0313).

3. "Investigation and Evaluation of Stress Corrosion Cracking in Piping of Light Water Reactor Plants," U.S. Nuclear Regulatory Commission, May 1979 (NUREG-0531).

4. E. Kiss, J. D. Heald, and D. A. Hale, "Low Cycle Fatigue of Prototype Piping," General Electric Company, January 1970 (GEAP-10135).

5. R. M. Horn, et al., "The Growth and Stability of SCC in Large Diameter BWR Piping," General Electric Company, December 1979 (NEDC-24750-1).

6. R. M. Horn, et al., "The Growth and Stability of SCC in Large Diameter BWR Piping," General Electric Company, June 1980 (NEDC-24750-2).

7. R. M. Horn, et al., "The Growth and Stability of SCC in Large Diameter BWR Piping," General Electric Company, December 1980 (NEDC-24750-3).

8. H. Tada, P. Paris, and R. Gamble, "Stability Analysis of Circumferential Cracks in Reactor Piping Systems," U.S. Nuclear Regulatory Commission, February 1979 (NUREG/CR0838).

9. K. H. Cotter, et al., "The Application of Tearing Modulus Stability Concepts to Nuclear Piping," Final Report, November 1981 (EPRI Project T118-9).

10. "Mechanical Fracture Predictions for Sensitized Stainless Steel Piping with Circumferential Cracks," Final Report, September 1975 (EPRI Report NP-192).

11. "Review and Assessment of Research Relevant to Design Aspects of Nuclear Power Plant Piping Systems," Nuclear Regulatory Commission, July 1977 (NUREG-0307).

12. M. B. Reynolds, "Failure Behavior of Flawed Carbon Steel Pipes and Fitting," AEC Research and Development Report, General Electric Company, October 1970 (GEAP-10236).

13. E. Smith, "Theoretical Justification of the Association of a Critical Net-Section Stress with Fracture Initiation at a Crack Tip," Int'l. J. of Pressure Vessels and Piping, Vol. 8, 4, July-Aug. 1980, pp. 303-311.

14. R. P. Harrison, K. Loosemore, and I. Milne, 1976, "Assessment of the Integrity of Structures Containing Defects," C.E.G.B. Report No. R/H/R 6.

15. R. J. Eiber, et al., "Review of Through-Wall Critical Crack Formulations for Piping and Cylindrical Vessels," May 1970 (Battelle Memorial Institute Report BMI 1883).

16. C. B. Buchalet and W. H. Bamford, "Stress Intensity Factor Solutions for Continuous Surface Flaws in Reactor Pressure Vessels," American Society for Testing and Materials, 1976 ASTM STP 590, pp. 385-402.

17. R. M. Horn, et al., "Crack Growth Behavior of Sensitized Stainless Steel in High Temperature High Purity Oxygenated Water," IAEA Conference, Freiburg, Germany, May 1981.

18. K. M. Douglas, General Electric Company, private communication.

Table 1

SUMMARY RESULTS OF NONLINEAR DYNAMIC ANALYSIS OF THE PIPING SYSTEM FOR VARIOUS FLAW CONFIGURATIONS, FLAW LOCATIONS, AND SEISMIC CONDITIONS

Flaw Configuration	Location	OBE Time-History Scaling Factor	Maximum Absolute Moment from Elastic Analysis, M_e (in.-lbf)	Maximum Absolute Moment from Elastic-Plastic Analysis, M_{ep} (in.-lbf)	Ratio M_e/M_{ep}
$\alpha/\pi = 1.0$ $a/t = 0.67$	Elbow	10.0	2.0×10^6	1.29×10^6	1.55
$\alpha/\pi = 1.0$ $a/t = 0.67$	Safe-End	10.0	4.3×10^6	2.08×10^6	2.07
$\alpha/\pi = 0.5$ $a/t = 1.0$	Elbow	5.0	1.0×10^6	0.55×10^6	1.82
$\alpha/\pi = 0.5$ $a/t = 1.0$	Safe-End	5.0	2.15×10^6	0.9×10^6	2.39
$\alpha/\pi = 0.5$ $a/t = 1.0$	Safe-End	2.5	1.08×10^6	0.64×10^6	1.69

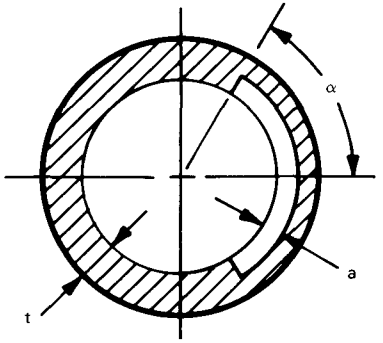

Table 2

ACCEPTANCE FLAW SIZE FOR NORMAL CONDITIONS

	Ratio of Length to Circumference $\ell/2\pi r$				
$\frac{P_m+P_b}{S_m}$	0.1	0.2	0.3	0.4	0.5 or more
	a/t				
1.4	0.50	0.40	0.30	0.20	0.10
1.3	0.58	0.48	0.38	0.28	0.18
1.2	0.66	0.56	0.46	0.43	0.26
1.1	0.73	0.63	0.53	0.36	0.33
1.0	0.75	0.70	0.60	0.50	0.40
0.9	0.75	0.75	0.66	0.56	0.46
0.8	0.75	0.75	0.70	0.60	0.50

Table 3

ACCEPTANCE FLAW SIZE FOR FAULTED CONDITIONS

	$\ell/2\pi r$				
$\frac{P_m+P_b}{S_m}$	0.1	0.2	0.3	0.4	0.5 or more
	a/t				
2.8	0.50	0.40	0.30	0.20	0.10
2.6	0.58	0.48	0.38	0.28	0.18
2.4	0.66	0.56	0.46	0.36	0.26
2.2	0.73	0.63	0.53	0.43	0.33
2.0	0.75	0.70	0.60	0.50	0.40
1.8	0.75	0.75	0.66	0.56	0.46
1.6	0.75	0.75	0.70	0.60	0.50

Table 4

STRESSES - 10-in. SCHEDULE 80 RECIRCULATION RISER

Stress Type	Axial Component
A. Primary	6.07 ksi
B. Secondary	18.51 ksi
C. Residual (linear)	40 ksi i.d., 0 - Neutral axis -40 ksi, o.d.

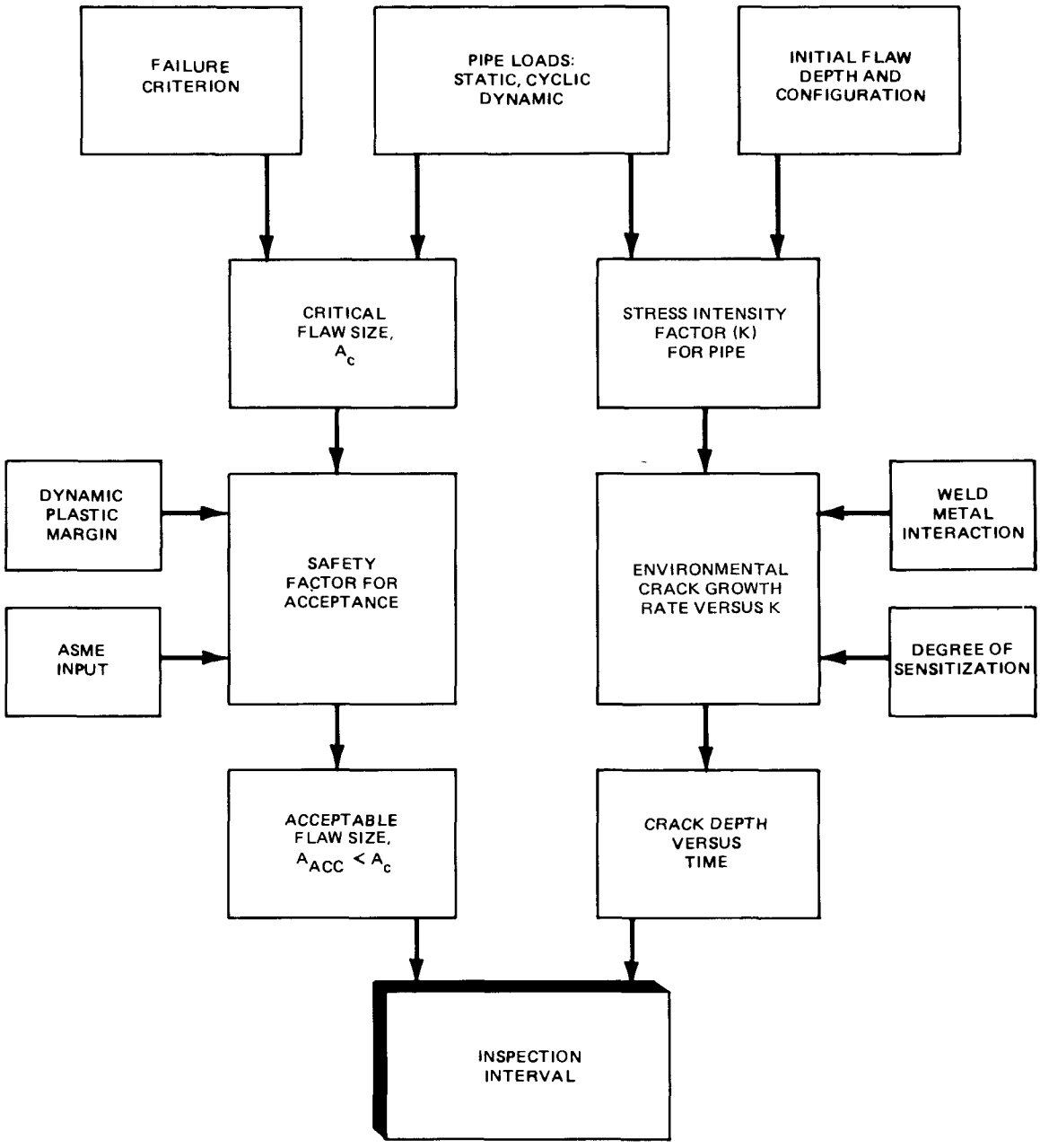

Figure 1. Flow Chart of Predictive Methodology (with left vertical path used to determine acceptable flaw size and right vertical path used to determine crack growth as a function of time)

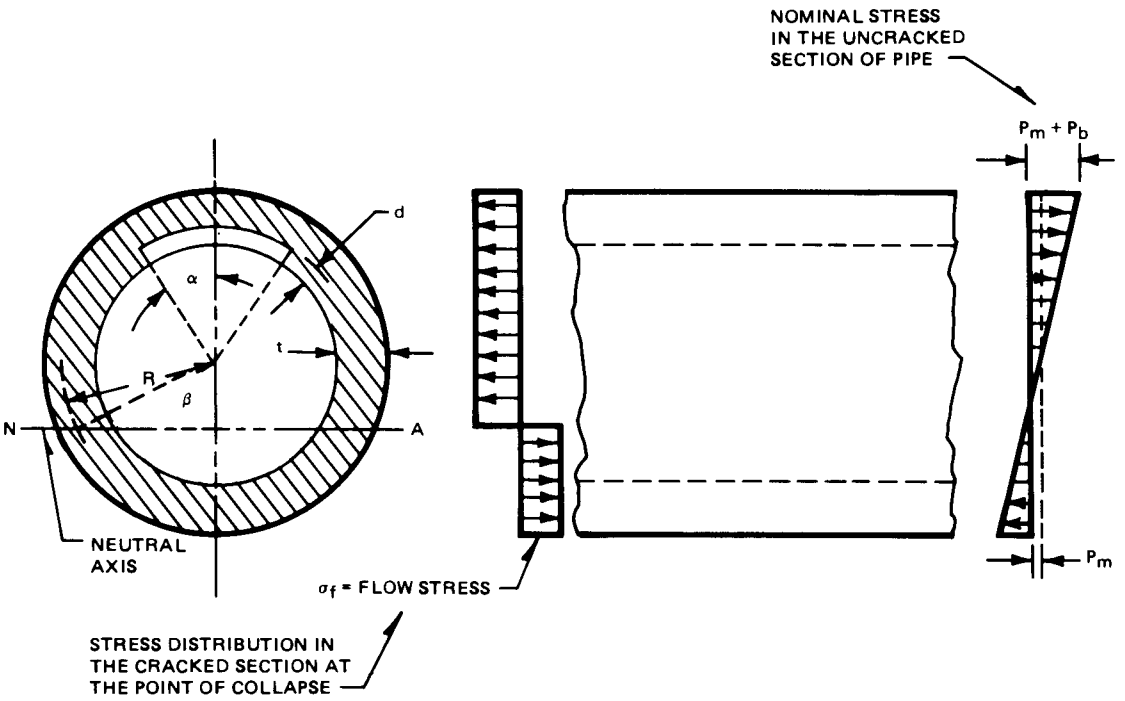

Figure 2. Schematic Showing Stress Distributed in a Cracked Pipe at the Point of Collapse

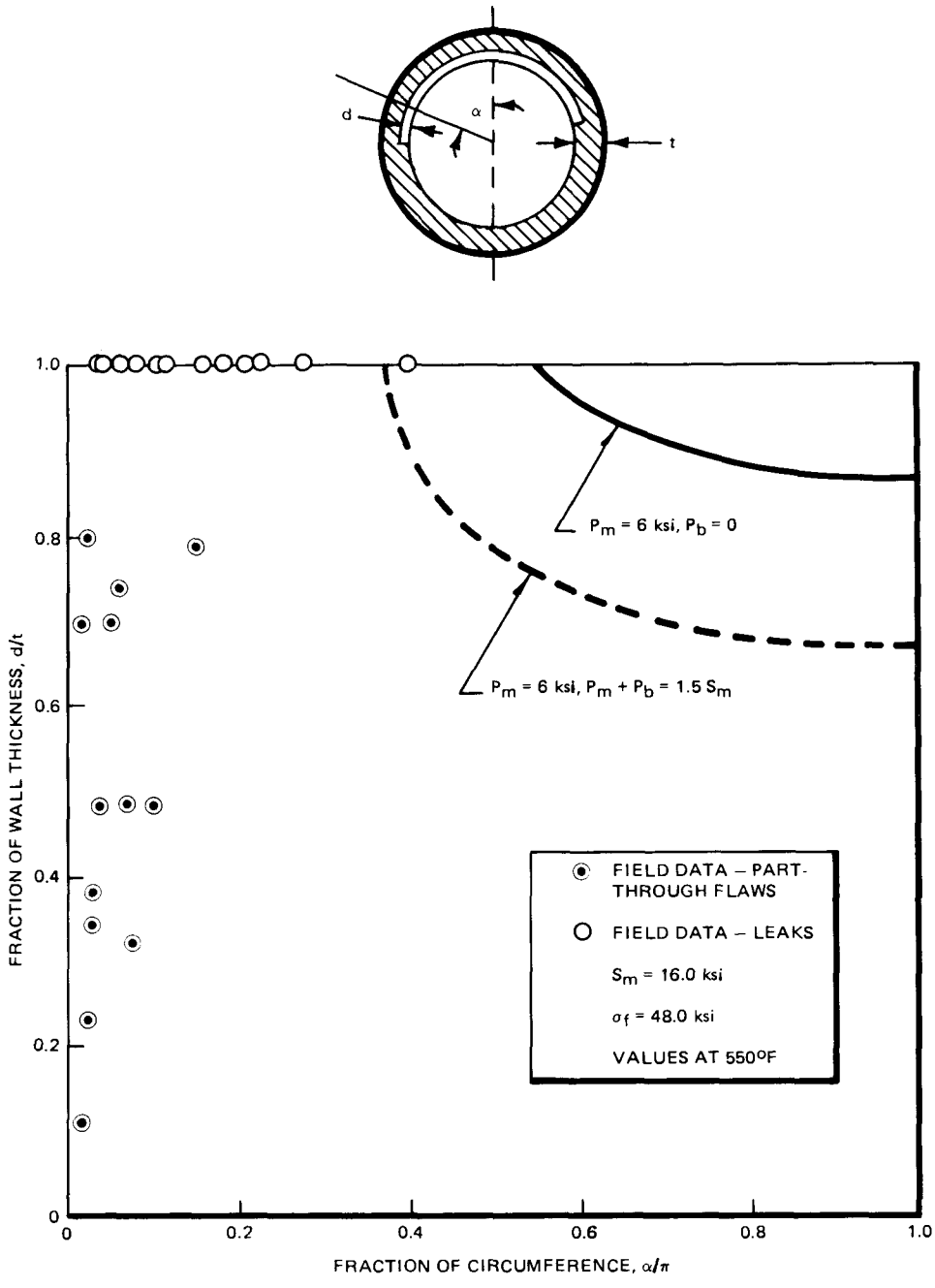

Figure 3. Comparison with Field Data - Stainless Steel Piping

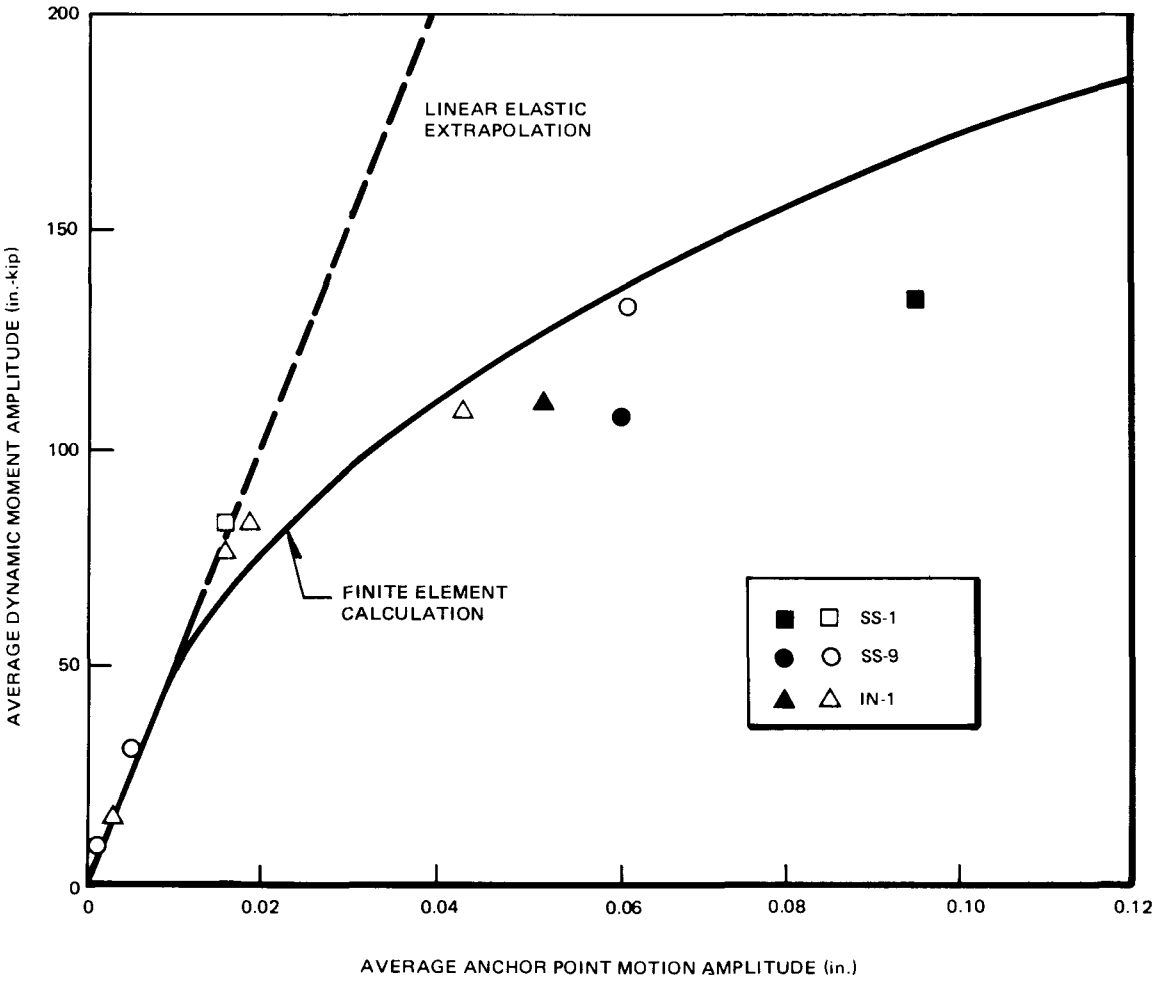

Figure 4. Comparison of Dynamic Pipe Test Results to Elastic-Plastic Dynamic Analysis-Predicted Response, 2/3 x 360-in. Flaw, f_n = 12 Hz. (Open symbols are no failure, solid points represent final failure.)

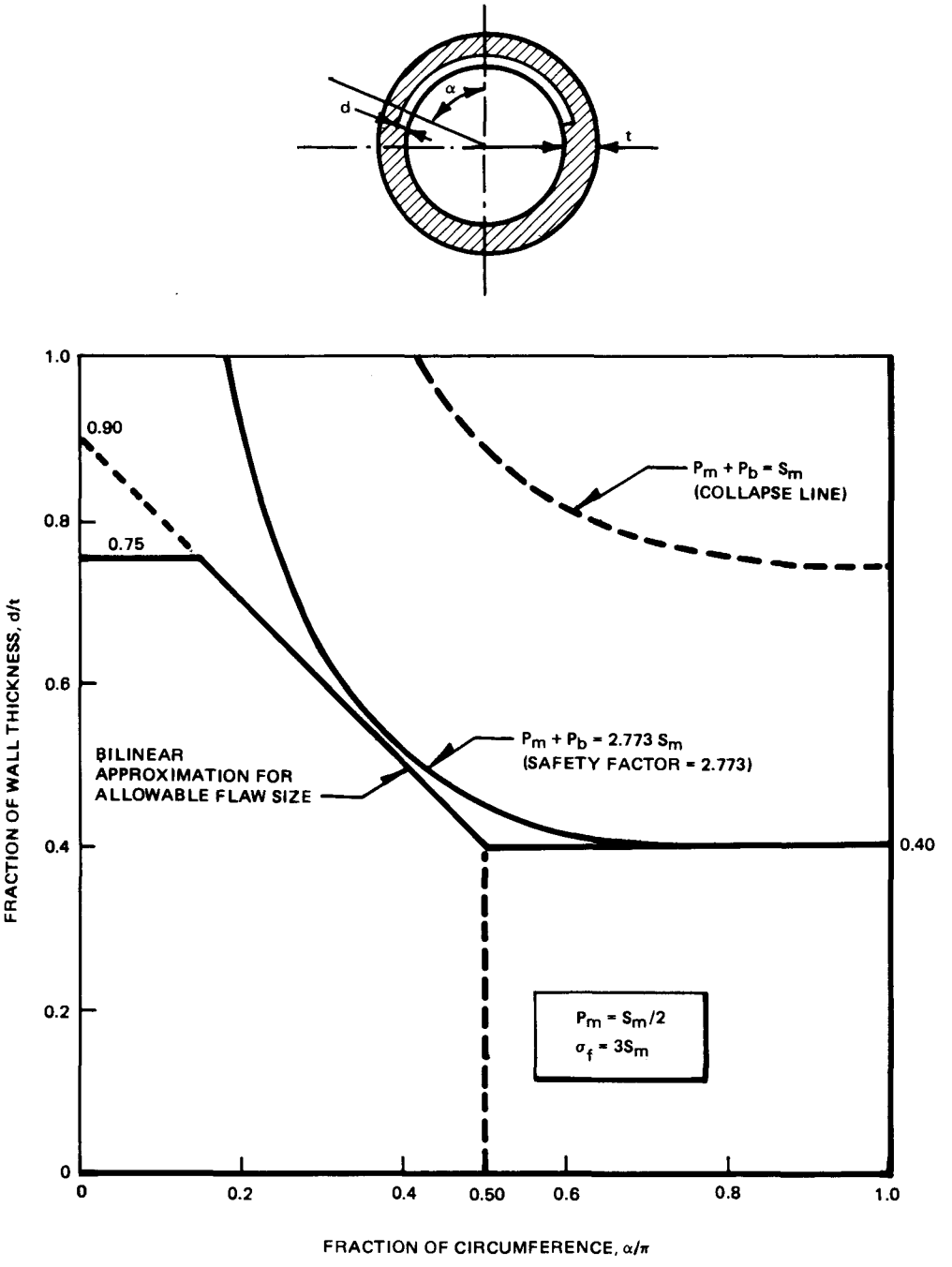

Figure 5. Determination of Allowable Flaw Sizes with a Safety Factor of 2.773 for Normal Conditions

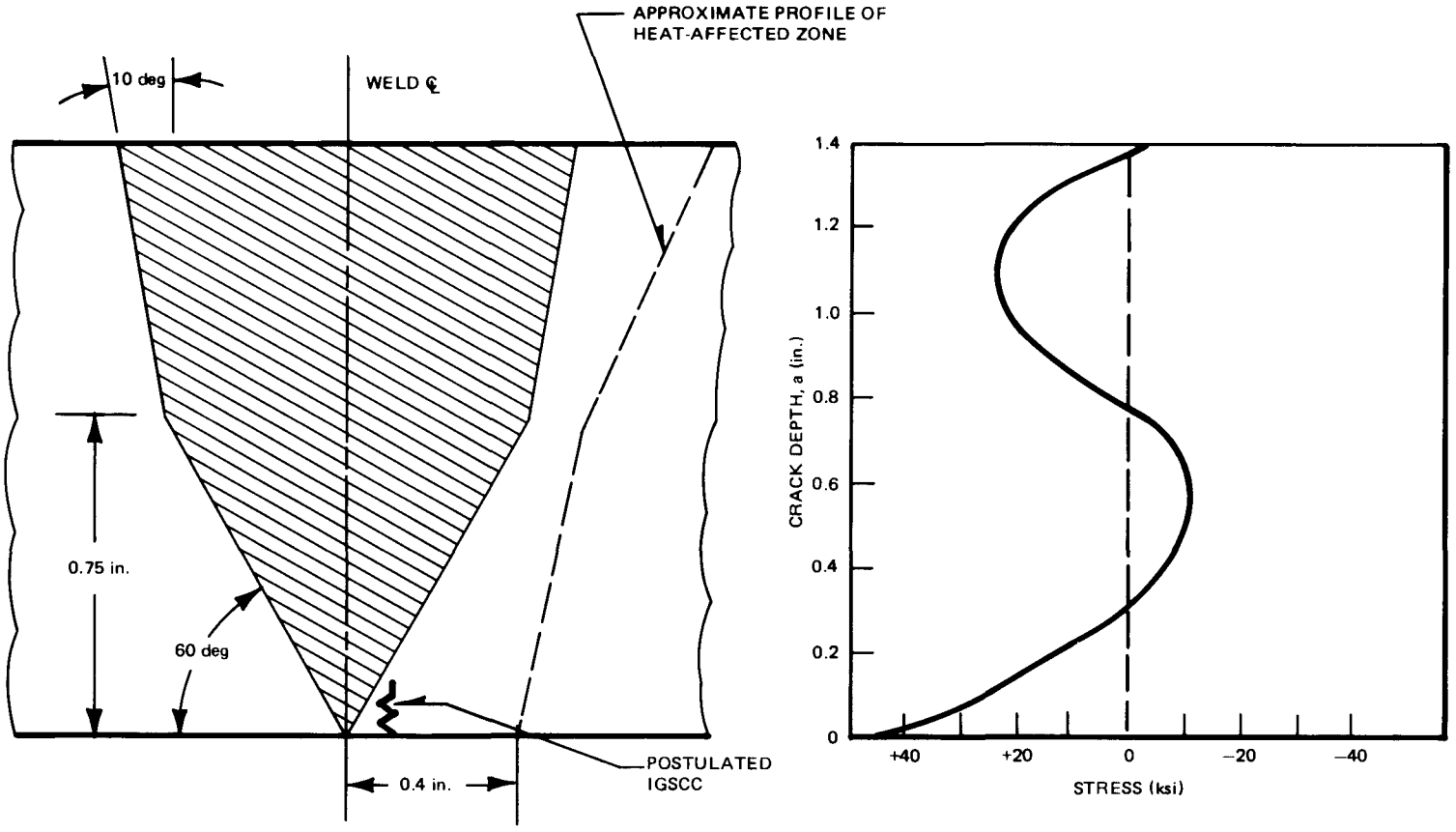

Figure 6. Schematic of Large Diameter Pipe
(a) Through-wall schematic showing weld area with postulated intergranular crack located adjacent to fusion line
(b) Through-wall axial stress at plane of crack

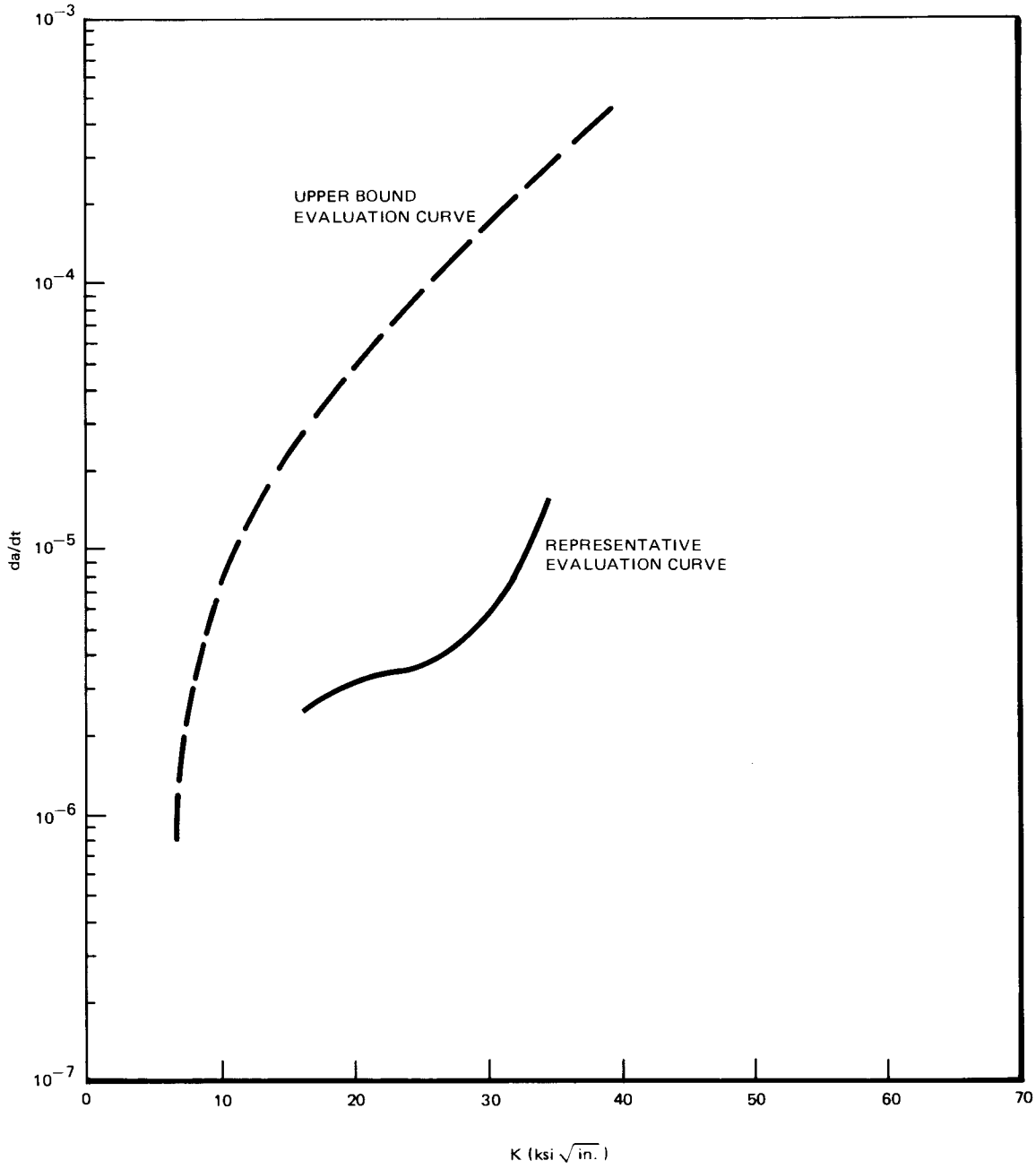

Figure 7. Upper Bound Evaluation Curve and Representative Evaluation Curve Used to Evaluate Crack Growth Behavior. The Curves Are Based on Constant Load Crack Growth Test Results Presented in Appendix H.

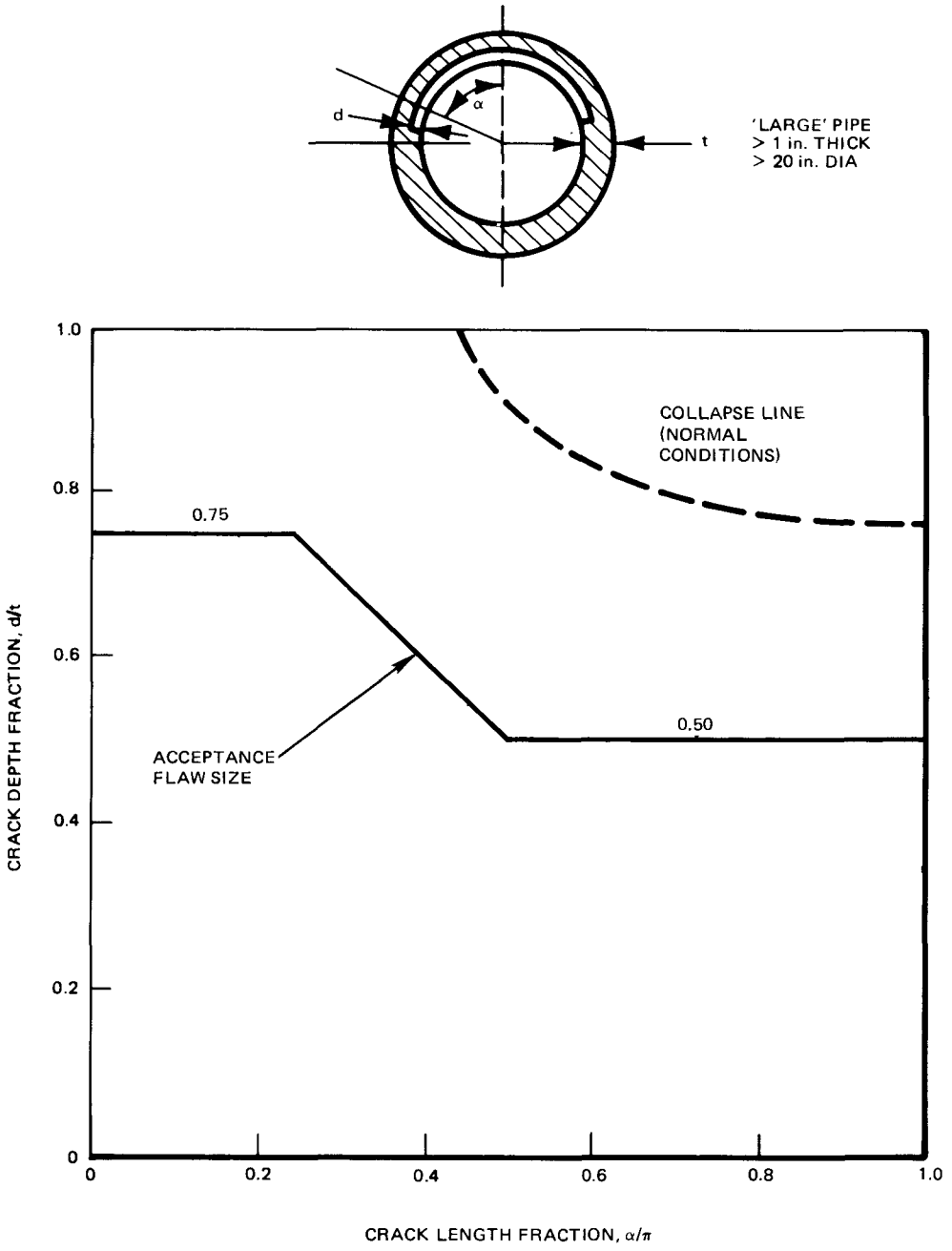

Figure 8. Acceptance Criteria for Flaw in Cracked Large Diameter Piping. Determined from Table 2 for $P_m + P_b = 0.8S_m$.

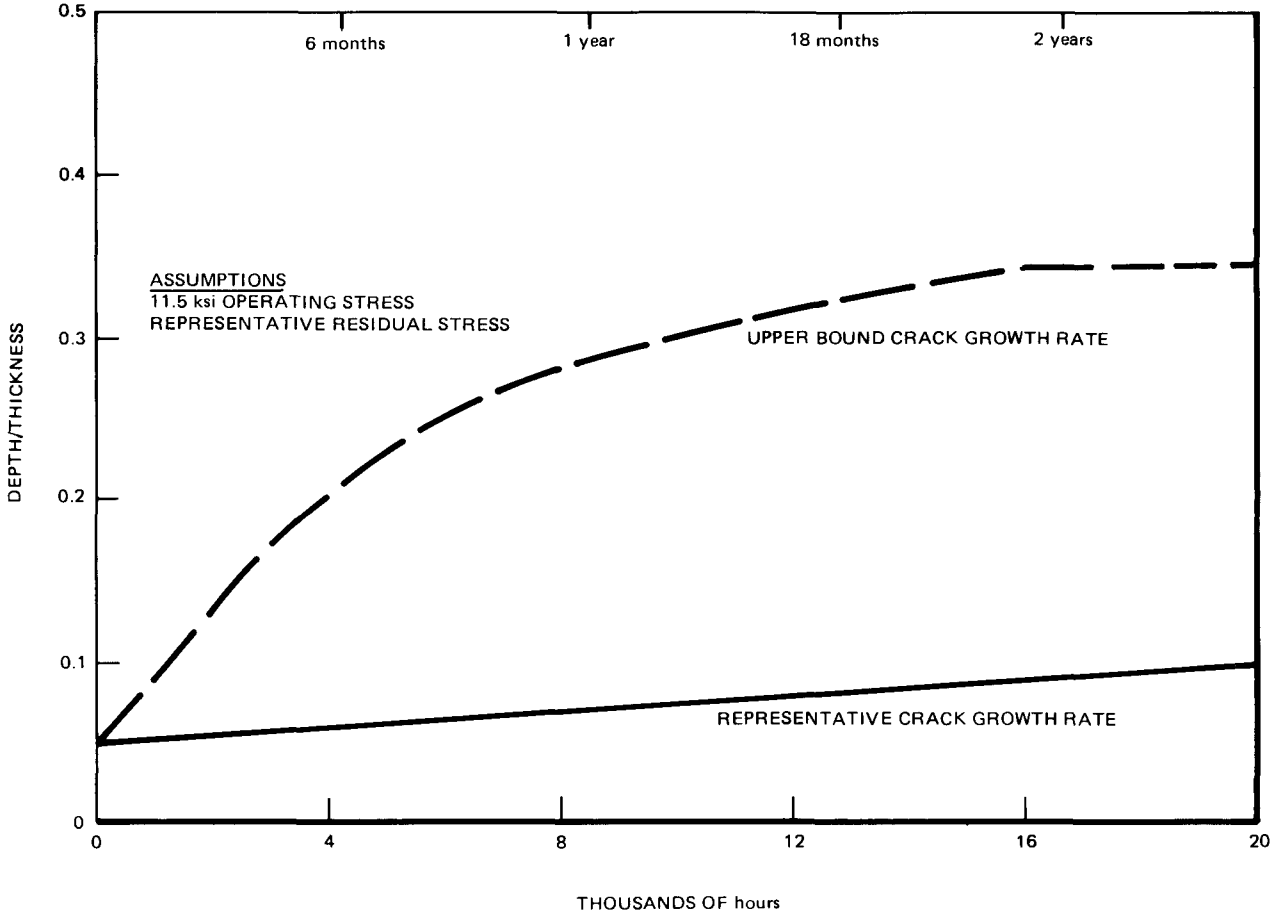

Figure 9. Depth versus Time Predictions for Large Pipe Comparing Representative and Upper Bound Crack Growth Rates. (Crack growth is expected to stop because (1) stress intensity decreases below threshold value and (2) crack intersects weld metal which is resistant to IGSCC.)

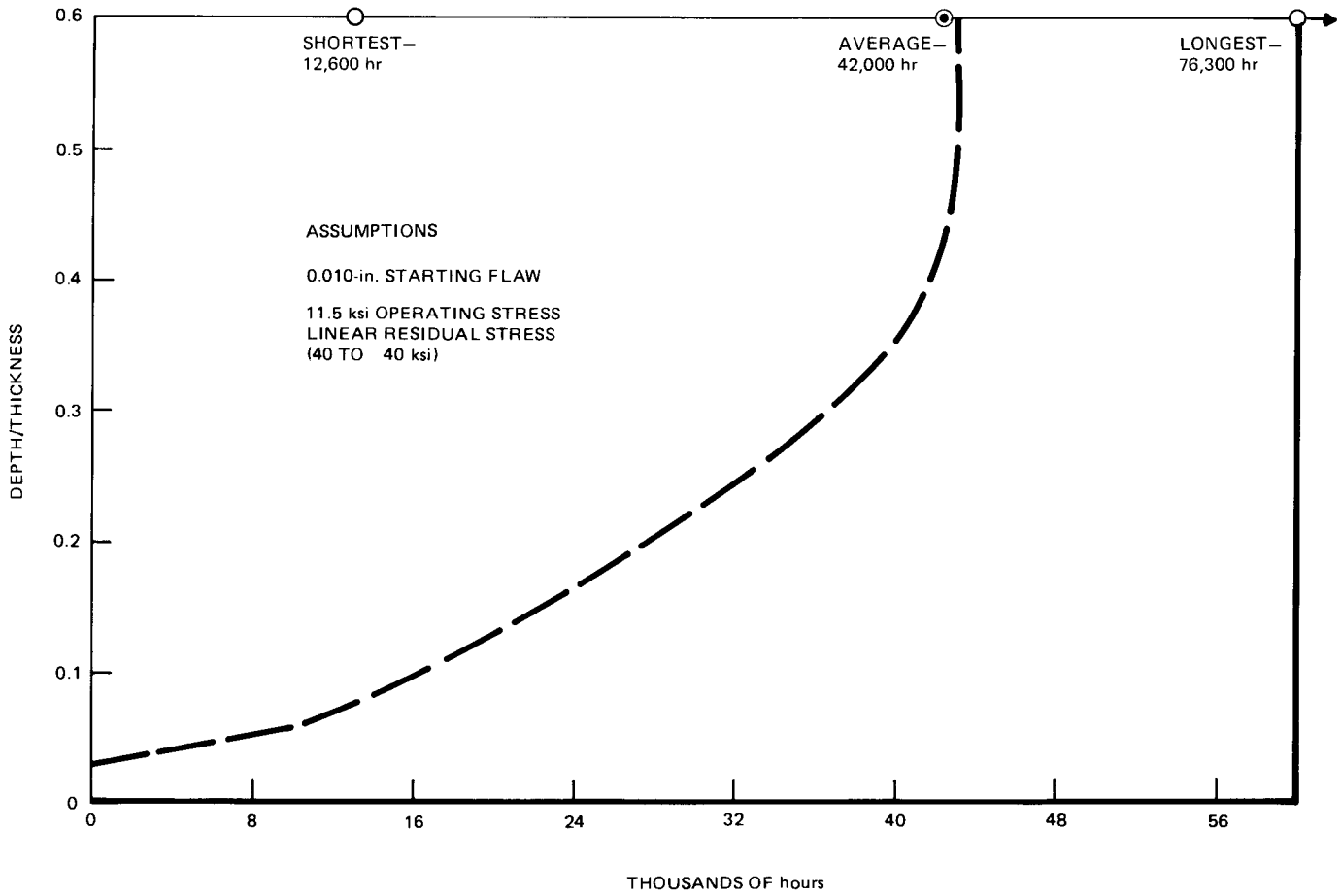

Figure 10. Predictions of 4-in. Schedule 80 Pipe Behavior Using Representative Crack Growth Rates (Normal operating conditions and residual stress assumed. Data on field through-wall cracking incidents used.)

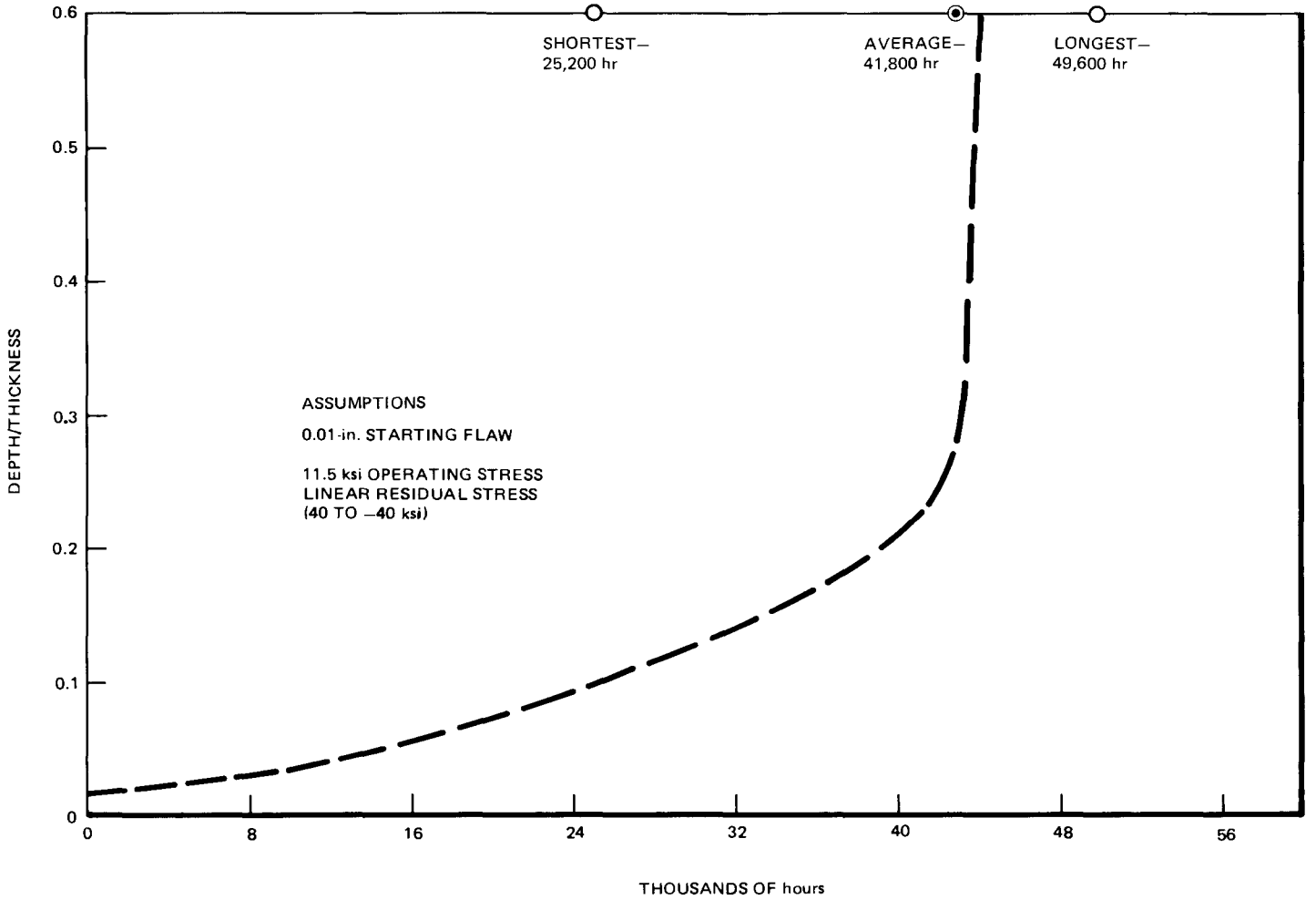

Figure 11. Prediction of 10-in. Schedule 80 Pipe Behavior Using Representative Crack Growth Rates (Normal operating residual stresses assumed. Data on field through-wall cracking incidents used.)

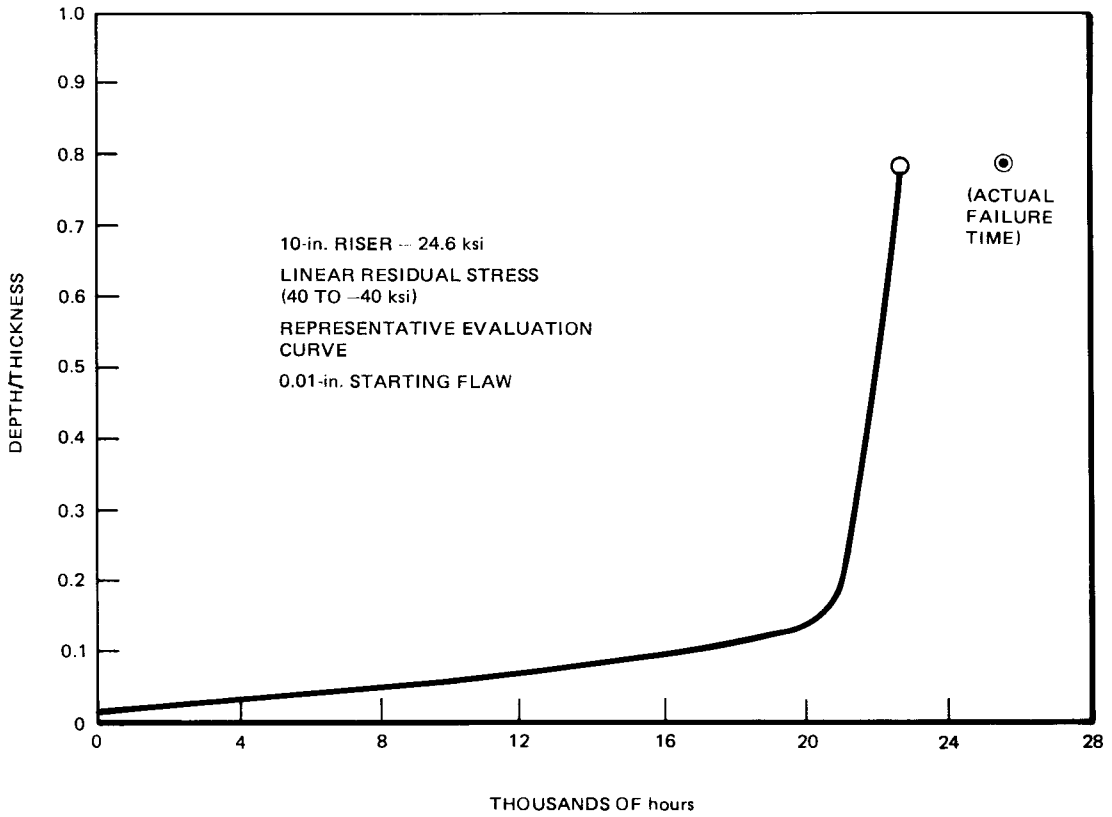

Figure 12. Prediction of 10-in. Recirculation Riser Behavior (Actual operating stresses used with representative crack growth rates.)

EPRI NP-2472-SY, Vol 1

Below are five index cards that allow for filing according to the four cross-references in addition to the title of the report. A brief abstract describing the major subject area covered in the report is included on each card.

EPRI NP-2472-SY
Volume 1
RPT118-1
Final Report
July 1982

The Growth and Stability of Stress Corrosion Cracks in Large-Diameter BWR Piping
Volume 1: Summary

Contractor: General Electric Company

Results of a research program conducted to evaluate the behavior of hypothetical stress corrosion cracks in large-diameter piping are reviewed. Details of the program, which included major tasks, a design margin assessment, an evaluation of crack growth and crack arrest, and development of a predictive model, are summarized. Volume 1 reports the research in a summary paper format. 54 pp.

EPRI Project Manager: D. M. Norris

Cross-References:
1. EPRI NP-2472-SY, Volume 1 2. RPT118-1 3. BWR Owners Group 4. Crack Growth

ELECTRIC POWER RESEARCH INSTITUTE
Post Office Box 10412, Palo Alto, CA 94303 415-855-2000

EPRI NP-2472-SY, VOLUME 1

EPRI NP-2472-SY
Volume 1
RPT118-1
Final Report
July 1982

The Growth and Stability of Stress Corrosion Cracks in Large-Diameter BWR Piping
Volume 1: Summary

Contractor: General Electric Company

Results of a research program conducted to evaluate the behavior of hypothetical stress corrosion cracks in large-diameter piping are reviewed. Details of the program, which included major tasks, a design margin assessment, an evaluation of crack growth and crack arrest, and development of a predictive model, are summarized. Volume 1 reports the research in a summary paper format. 54 pp.

EPRI Project Manager: D. M. Norris

Cross-References:
1. EPRI NP-2472-SY, Volume 1 2. RPT118-1 3. BWR Owners Group 4. Crack Growth

ELECTRIC POWER RESEARCH INSTITUTE
Post Office Box 10412, Palo Alto, CA 94303 415-855-2000

RPT118-1

EPRI NP-2472-SY
Volume 1
RPT118-1
Final Report
July 1982

The Growth and Stability of Stress Corrosion Cracks in Large-Diameter BWR Piping
Volume 1: Summary

Contractor: General Electric Company

Results of a research program conducted to evaluate the behavior of hypothetical stress corrosion cracks in large-diameter piping are reviewed. Details of the program, which included major tasks, a design margin assessment, an evaluation of crack growth and crack arrest, and development of a predictive model, are summarized. Volume 1 reports the research in a summary paper format. 54 pp.

EPRI Project Manager: D. M. Norris

Cross-References:
1. EPRI NP-2472-SY, Volume 1 2. RPT118-1 3. BWR Owners Group 4. Crack Growth

ELECTRIC POWER RESEARCH INSTITUTE
Post Office Box 10412, Palo Alto, CA 94303 415-855-2000

BWR OWNERS GROUP

EPRI NP-2472-SY
Volume 1
RPT118-1
Final Report
July 1982

The Growth and Stability of Stress Corrosion Cracks in Large-Diameter BWR Piping
Volume 1: Summary

Contractor: General Electric Company

Results of a research program conducted to evaluate the behavior of hypothetical stress corrosion cracks in large-diameter piping are reviewed. Details of the program, which included major tasks, a design margin assessment, an evaluation of crack growth and crack arrest, and development of a predictive model, are summarized. Volume 1 reports the research in a summary paper format. 54 pp.

EPRI Project Manager: D. M. Norris

Cross-References:
1. EPRI NP-2472-SY, Volume 1 2. RPT118-1 3. BWR Owners Group 4. Crack Growth

ELECTRIC POWER RESEARCH INSTITUTE
Post Office Box 10412, Palo Alto, CA 94303 415-855-2000

CRACK GROWTH

EPRI NP-2472-SY
Volume 1
RPT118-1
Final Report
July 1982

The Growth and Stability of Stress Corrosion Cracks in Large-Diameter BWR Piping
Volume 1: Summary

Contractor: General Electric Company

Results of a research program conducted to evaluate the behavior of hypothetical stress corrosion cracks in large-diameter piping are reviewed. Details of the program, which included major tasks, a design margin assessment, an evaluation of crack growth and crack arrest, and development of a predictive model, are summarized. Volume 1 reports the research in a summary paper format. 54 pp.

EPRI Project Manager: D. M. Norris

Cross-References:
1. EPRI NP-2472-SY, Volume 1 2. RPT118-1 3. BWR Owners Group 4. Crack Growth

ELECTRIC POWER RESEARCH INSTITUTE
Post Office Box 10412, Palo Alto, CA 94303 415-855-2000